

NUMERICAL AND EXPERIMENTAL INVESTIGATIONS OF DRAG FORCE ON SCALED CAR MODEL

by

Selvaraju PONNUSAMY NALLUSAMY^{a*}
and Parammasivam KANJIKOVIL MAHALI^b

^a Department of Automobile Engineering, Rajalakshmi Engineering College, Chennai, India

^b Department of Aerospace Engineering, MIT, Anna University, Chennai, India

Original scientific paper
DOI: 10.2298/TSCI16S4153P

The numerical simulation and wind tunnel experiment were involved to observe the aerodynamic characteristics of car model. The investigation of aerodynamic characteristics on car model were difficult by using wind tunnel. It provides more comprehensive experimental data as a reference to validate the numerical simulation. In the wind tunnel experiments, the pressures on various ports over the car model were measured by using pressure scanner (64 bit channels). The drag force was calculated based on experimental and computational results. The realizable $k-\epsilon$ model was employed to compute the aerodynamic drag and surface pressure distribution over a car model simulated at various wind velocity. The tetrahedron mesh approach was used to discretize the computational domain for accuracy. The computational results showed a good agreement with the experimental data and the results revealed that the induced aerodynamic drag determines the best car shape. In order to reveal the internal connection between the aerodynamic drag and wake vortices, the turbulent kinetic, re-circulation length, position of vortex core, and velocity profile in the wake were investigated by numerical analysis.

Key word: *wind tunnel, CFD, wake region, pressure scanner, turbulence*

Introduction

Aerodynamics was first introduced to increase stability in race cars. Race car engineers realized that air flowing around the vehicle could be used to increase down force and reduce aerodynamic drag on the car. Then they realized that the drag affects fuel economy in road vehicle design. So the method could be transferred to reduce aerodynamic drag on to road vehicles in order to improve fuel economy. To decrease the amount of drag created by a vehicle, automobile manufacturers began incorporating vehicle body designs that would allow the vehicle to be more streamlined. Methods of decreasing the drag coefficient of a vehicle include modifying shape of the rear end, base bleed covering the underside of the vehicles, and reducing the amount of projections on the outer surface of the car. Birwa *et al* [1], found that the drag coefficient decreases with the velocity increasing from 30 to 60 m/s and increases with the ground clearance from 101.6 mm to 152.4 mm. Song *et al* [2], found that from the result of CFD, the parts from the end of the sedan were chosen as the design variables for optimization. Littlewood

* Corresponding author; e-mail: selvarajumit@yahoo.co.in

and Passmore [3] investigated that the effects of the steady blowing on the vehicle wake structures affect drag dominantly. Sai Sijith and Ravindra Reddy [4] concluded the flow separation takes in upstream of the vehicle. Manan Desai *et al.* [5] revealed that the computed drag forces and pressure distributions concurrence well with the experimentl values over the whole range of air velocities. Tsubokura [6] investigated that formation of eddies varied around the vehicle and causes for overall aerodynamic characteristics of the vehicle. Hu *et al.* [7] concluded that when the diffuser angle increases, the underbody flow and especially the wake change greatly and the pressure changes correspondingly. Itsuhei *et al.* [8] analyzed that wake structure of Ahmed car model due to unsteady characteristics Khaled, *et al* [9], described that the most crucial parameters in new car development is the aerodynamic torsor of a vehicle. This torsor has been used to reduce drag on car profile significantly. Vino *et al.* [10] concluded that the wake region on Ahmed car model can be studied by time average and time dependent system. Time dependant analysis is suitable to study the vortex shedding behind the bluff bodies than the time averaged system.

As mentioned previously, aerodynamic drag is the force that opposes the direction of thrust of a car and is not a desirable force. Given a set of vehicle conditions, the drag force can be calculated. Drag is a function of the frontal area of the vehicle, the density of the air, the coefficient of drag of the vehicle, and the vehicle speed squared. The effects of drag on a vehicle become even more prominent. However, when the engine power needed to overcome drag forces is realized. The engine power needed as a function of drag depends on the frontal area of the car, the density of the air, the coefficient of drag of the vehicle, and the vehicle speed. The fact that the vehicle speed has a cubic relation to the force of drag reveals that a small change in the speed of the car requires an enormous amount of engine power to overcome the forces of drag. In addition, the relation between drag and speed shows that aerodynamics of vehicles do not matter so much at lower speeds. They have a much more intense effect at higher speeds. However, the air that flows around the car swirls around the rear much more for the actual vehicle profile as compared with the teardrop profile. These swirls around the rear are called vortices, and they represent a low-pressure area behind the car. The low pressure behind the car creates a suction effect that tries to pull the vehicle backwards. Therefore, reducing the size of the separation zone, which is the area behind the car containing the vortices behind the car, is one of the predominant methods of decreasing aerodynamic drag. This can be done by slightly tapering the rear end of a car to reduce the size of the separation zone.



Figure 1. Open type subsonic wind tunnel

Experimental set-up

The aerodynamic study of the car model of scale ratio 1:12 was employed using subsonic suction type wind tunnel. The subsonic wind tunnel facility can be viewed as an experimental facility. The wind flow is simulated in a controlled manner to represent the flow characteristics in the nature and the aerodynamic forces. The responses of the model are investigated in a scientific manner. The subsonic wind tunnel comprises of honey comb, contraction chamber, test section, and diffuser.

The open type subsonic wind tunnel, fig. 1, is utilized in this work with test cross-section is about $1.2 \text{ m} \times 1 \text{ m}$ and maximum speed of

blower is about 150 rpm with consuming input power of 170 HP, 415 V, respectively. The blockage ratio of wind tunnel is defined as the ratio of frontal area of the model to wind tunnel inlet test section area and it should not exceed 7.5%. The blockage ratio is calculated as 2.2% for this case since it is within the specified limit so model can be suitably tested in this test section configuration.

Scaled car model

The pressure tubes were connected to the port which was drilled around the car model, fig. 2. The other ends of the tubes are connected with the ports available in the pressure scanner (64 bit). The pressure scanner is connected with the computer which displayed pressure values around the car model by using predetermined software. The measurement is carried out with the different velocities of air and the pressure values were tabulated.

Electronic pressure scanners

Electronic pressure scanners (EPS) are miniature electronic differential pressure measurement units which consist of an array of silicon piezo-resistive pressure sensors, committed as one for each pressure port, fig. 3. The sensors are mounted on a common hybrid glass substrate using a proprietary technique which maximizes long term stability. The outputs of the sensors are electronically multiplexed through a single onboard instrumentation amplifier at rates up to 70,000 Hz using binary addressing. The multiplexed amplified analog output is capable of driving long lengths of cable to a remote A/D converter. The EPS scanners also incorporate a two position calibration manifold actuated by momentary pulses of control pressures. When placed in the calibrate position, all sensors are connected to a common calibration pressure port. A series of accurately measured pressures can be applied through this port to characterize the sensors.

Numerical simulation

The scaled car model was created by modeling software (Uni-Graphics) for computational as shown in fig. 4. The computational domain and pressure port points were created as similar experimental set-up as shown in figs. 5 and 7. The ANSYS fluent software was used for numerical simulation using boundary condition given in tab. 1. The tetrahedral mesh was used for computational domain to analyze force on the surface of the car model. The $k-\epsilon$ model was used to analysis turbulent and wake region on the car model. The turbulent kinetic energy and



Figure 2. Car model for experimental analysis

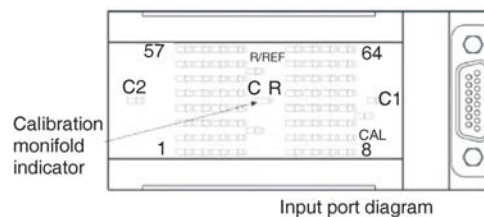


Figure 3. Electronic pressure scanners

C1 – indicator pin when run position, *C2* – indicator pin when calibration position, *CR* – calibration manifold indicator, *C/REF* – calibration reference port, *R/REF* – run reference port, *CAL* – calibration valve, 1 to 64 – pressure port



Figure 4. Geometry car model

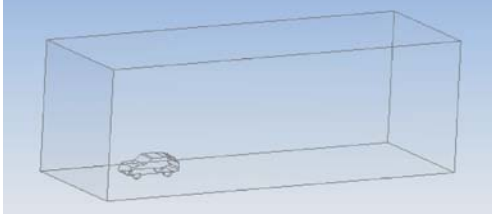


Figure 5. Computational domain on car model

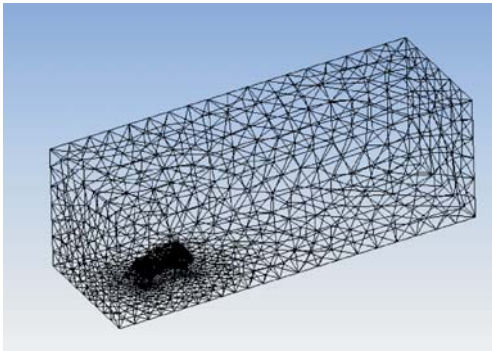


Figure 6. Mesh geometry

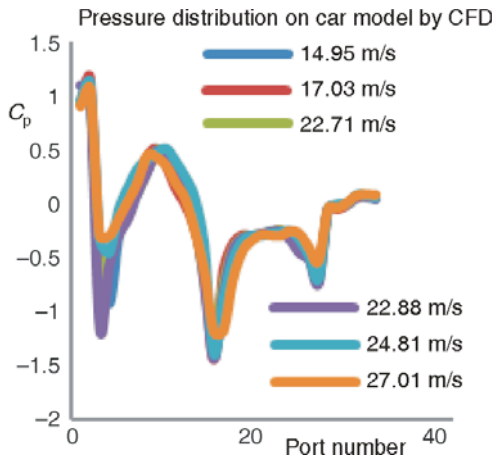


Figure 8. Pressure coefficient vs. port number

model. From the graph plotted experimentally and numerically, low pressure region induced on rear portion of the car for all speed, figs. 8 and 9. This influences drag induced on car model. Whereas in analytical results, the low pressure region started at tail end region of roof. Also the pressure distribution over the car model is plotted at various wind speeds.

The drag increases with velocity from both experimental and numerical, fig. 10. Also it is observed that at higher vehicle speed, drag affects on the vehicle performance dominantly.

Table 1. Boundary condition for CFD analysis

| Region | Boundary condition |
|-----------------|---|
| Inlet | Velocity, $V_{\max} = 27.01$ m/s Turbulent intensity = 1 % |
| Outlet | Pressure outlet, reference pressure = 0 Pa |
| Top and side | Wall and no slip |
| Ground | Wall and no slip |
| Turbulent model | $k-\epsilon$ model |

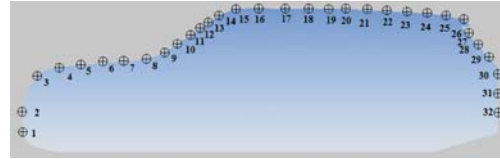


Figure 7. Ports on car model

turbulent dissipation were visible by second order upwind discretization method.

Calculation of drag coefficient and drag force

Drag coefficient $C_d = C_p \cos \theta s/h$ where C_p is the pressure coefficient, s – the length port, h – the height of the port, and θ – the angle at port.

Drag force $D = \frac{1}{2} C_d \rho V^2 A$ where V [ms^{-1}] is the velocity of air, C_d – the non-dimensional drag coefficient, A – the projected frontal area of the car model, and ρ – the density of the ambient air.

Result and discussion

The pressure coefficients at various ports on the car model were analyzed from the graph as shown in fig. 8. The flow patterns were studied over the car model both experimental and by analytical. It is clear that the pressure distribution varies with respect to various position of the car

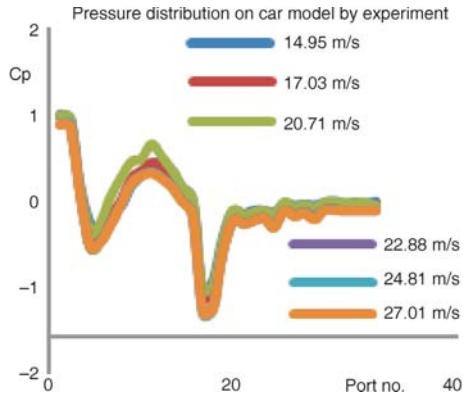


Figure 9. Pressure coefficient vs. port number

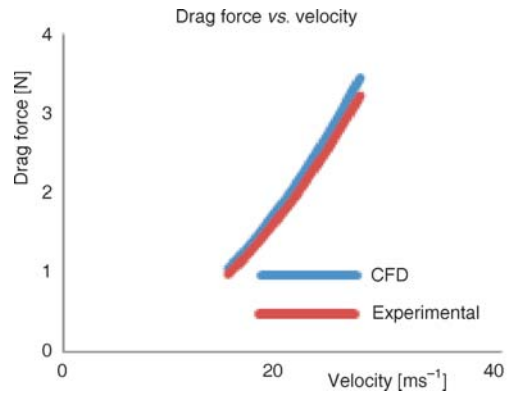


Figure 10. Drag vs. velocity

From the computational graphs, the turbulence induced by car model was noticed on rear region only, which causes the wake flow. The wake flow induces pressure drag, which affect the performance of vehicle. From fig. 11, the pressure contour on the car model analyzed. Flow separation on car profile also analyzed which is the cause for turbulence on the rear region of the car model. From fig. 12, the velocity contour over the car profile analyzed. From fig. 13 the velocity vector on car profile analyzed and turbulent flow measured. It is also observed from the fig. 14 that turbulent flow causes for swirling.

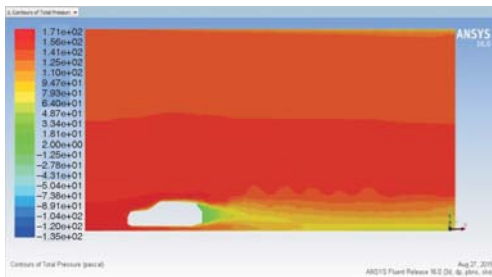


Figure 11. Contours of pressure distribution over the car model

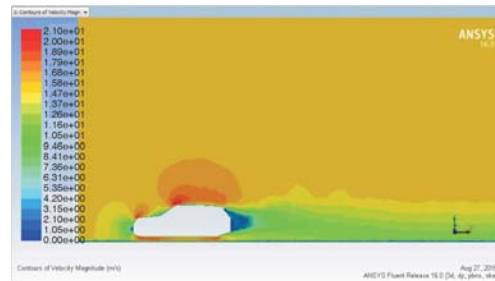


Figure 12. Contours of velocity

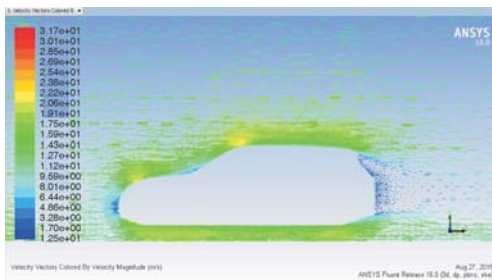


Figure 13. Velocity vectro on car model

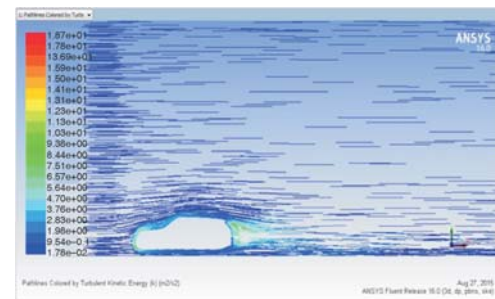


Figure 14. Turbulent on car model

Conclusion

The pressure distributions on car model were studied by experimental and validated with computational results. The drag coefficient on car model was 0.3414 by computational method and 0.3187 by experimental method. The boundary layer thickness analyzed on car model by computational and used to design vortex generator for further reducing drag force. The turbulent flow region, boundary layer separation and wake region were analyzed by computational performance result. All the results are obtained through experimental and numerical method are closely correlated with each other and this work will be the benchmark for further aerodynamic analysis on any type of car body. The modification on existing car model, attachment and active devices on car model will be used to reduce drag further and improve vehicle performance.

References

- [1] Birwa, S. K., et al., Aerodynamic Analysis of Audi A4 Sedan Using CFD, *J. Inst. Eng. India Ser. C*, 94 (2013), 2, pp. 105-111
- [2] Song, K. S., et al., Aerodynamic Design Optimization of Rear Body Shapes of a Sedan for Drag Reduction, *International Journal of Automotive Technology*, 13 (2012), 6, pp. 905-914
- [3] Littlewood, R. P., Passmore, M. A., Aerodynamic Drag Reduction of a Simplified Square Back Vehicle Using Steady Blowing, *Exp Fluids*, 53 (2012), 2, pp. 519-529
- [4] Sai Sujith, K., Ravindra Reddy, G., CFD Analysis of Sedan Car with Vortex Generators, *International Journal of Mechanical Engineering Applications Research*, 3 (2012), 3, pp. 179-184
- [5] Manan Desai, S., et al., Experimental and Computational Aerodynamic Investigations of a Car, *Wseas Transactions on Fluid Mechanics*, 4 (2008), 3, pp. 359-368
- [6] Tsubokura, M., et al., Computational Visualization of Unsteady Flow Around Vehicles Using High Performance Computing, *Computers & Fluids*, 38 (2009), 5, pp. 981-990
- [7] Hu, et al., Effect of Turbulence Parameters on Numerical Simulation of Complex Automotive External Flow Field, *Applied Mechanics and Materials*, 52-54 (2011), Mar., pp 1062-1067
- [8] Itsuhei, K., et al., Unsteady Characteristics of the Wake Structure of Ahmed Bluff Body, *Proceedings*, 4th International Conference on Jets, Wakes and Separated Flows, Berlin, 2013
- [9] Khaled, M., et al., Some Innovative Concepts for Car Drag Reduction: A Parametric Analysis of Aerodynamic Forces on a Simplified Body, *Journal of Wind Engineering and Industrial Aerodynamics*, 107-108 (2012), Aug.-Sep., pp. 36-47
- [10] Vio, G., et al., Flow Structures in the Near-Wake of the Ahmed Model, *Journal of Fluids and Structures*, 20 (2005), 5, pp. 673-695